Research Article Wiley Online Library ELECTROANALYSIS

doi.org/10.1002/elan.202100520

Electrochemical Detection of Phenol Removal by Using a Biosorbent Originated Factory Solid Waste

Gulsah Congur*[a, b] and Ülküye Dudu Gül*[b, c]

Abstract: Biosorption is a preferable method for phenol (PNL) removal from water sources using a cheap and eco-friendly biomass. The combination of the biosorption technique with practical, affordable, sensitive, and selective monitoring tools gives a new perspective to environmental monitoring applications. Herein, as the first time, the monitoring of PNL biosorption performed using a factory waste was done by pencil graphite electrodes (PGEs) and cyclic voltammetry (CV) technique. The monitoring of the biosorption process was completed with reproducible and reliable results in just 40s. The biosorption was achieved in different water samples and the presence of different phenolic compounds.

Keywords: Biosorption · Phenol · Pencil graphite electrode · Cyclic voltammetry

1 Introduction

Phenol (PNL) is a chemical found naturally and as a result of human and industrial activities. With increasing environmental pollution in the last century, water resources are contaminated with phenolic compounds, and the carcinogenic and toxic factors related to the PNL contamination in the environmental resources are gradually increasing [1,2]. PNL easily pollutes water resources since its solubility in water is high. Discharging of industrial wastes without any treatment rapidly contaminates water sources with phenolic compounds. In addition, it can stay in the soil for 2–5 days and in water for more than 9 days, and its high concentrations can stay much longer in air and soil.

Sustainability gains importance in today's world where environmental pollution is tremendously increasing and water resources are decreasing. Therefore, the removal of PNL from water sources with sustainable solutions and the monitoring of the removal with sensitive, accurate, reliable and inexpensive tools is an urgent need.

Adsorbents are frequently used in the removal of PNL and its derivatives from water sources. The most used adsorbent is activated carbon, which has a very large surface area due to its porous structure [3,4]. However, more economical adsorbents need to be investigated.

In the results of the recent studies, it has been shown that various types of dried biological materials can be successfully used for PNL adsorption [5–7]. The adsorption using such biological materials is defined as "biosorption", and the adsorbents used for this purpose are defined as "biosorbents". In the removal of PNL from liquid media, biological treatment is more widely used compared to other treatment systems for several reasons such as being cheap and easily applicable [8].

Previous PNL removal studies were carried out using the High-Performance Liquid Chromatography (HPLC) method [9] which was a time-consuming and also energy-consuming technique compared to the sensor systems [10].

Electrochemical sensor technologies are widely applied to the environmental monitoring areas [11–16]. They provide to fabricate easy-to-use, eco-friendly and affordable monitoring systems that can detect the target molecule in a shorter time than conventional techniques such as HPLC, gas chromatography (GC), mass spectrometry, etc [17]. An electrochemical system is generally comprised of a working electrode, a reference electrode, and a counter electrode. Although there are many types of working electrodes, pencil graphite electrodes (PGEs) have single-use, cheap and labor-friendly structures and they allow designing sensitive and selective monitoring platforms due to their robust graphite form [18–22].

There are some reports in the literature whose topics are to combine biosorption/bioremediation principles and electrochemical detection strategies. As an example, Cao et al. reported a Cu^{2+}–Cu^{+}/biochar material for the detection of nitrite in water using an electrochemical

[a] G. Congur
Bilecik Seyh Edebali University,
Vocational School of Health Services,
11230 Bilecik, Turkey
E-mail: gulsah.congur@bilecik.edu.tr
[b] G. Congur, Ü. D. Gül
Bilecik Seyh Edebali University,
Biotechnology Application and Research Center,
11230, Bilecik, Turkey
E-mail: ulkuyedudugul@bilecik.edu.tr
[c] Ü. D. Gül
Bilecik Seyh Edebali University,
Faculty of Engineering .
Department of Bioengineering,
11230, Bilecik, Turkey

Supporting information for this article is available on the WWW under https://doi.org/10.1002/elan.202100520

detection route [23]. They used a waste eggshell membrane called biochar and adsorbed Cu^{2+} ions from wastewater using the biochar. Then, they applied pyrolysis to convert Cu^{2+} to Cu^{+} ions into the biochar. They modified the glassy carbon electrode (GCE) using the biochar and used this modified electrode for voltammetric detection of nitrite in mineral water, tap water, and sausage. GCE was required to apply cleaning and polishing steps for each electrochemical measurement due to GCE is not a disposable electrode. The prepared biochar was sonicated and then it could be modified at the surface of GCE. All these experimental steps resulted in the development of a biosensor system whose preparation is time consuming and labor-intensive.

A biomass-modified carbon paste electrode (CPE) was reported by Estrada- Aldrete and coworkers [24]. Spent coffee grounds (SCG) were used as the biomass and were chemically pretreated to activate carboxyl groups of the biomass. This biomass was mixed with graphite powder and this mixture was used for the preparation of CPE. Then, Pb^{2+} and Cd^{2+} ions were determined by using this modified electrode and differential pulse voltammetry (DPV) technique. It should be pointed out that the preparation of CPE required grinding and filling steps which were done by using extra chemical agents. Furthermore, it is hard to obtain the same quality and same structure at CPE for each filling, it heavily depends on the hand skill of the laboratory worker. The same disadvantages could be observed for the application of the electrochemical sensor system reported by Njanja et al. [25]. They developed an amperometric sensor for monitoring methylene blue (MB) biosorption performed by using coffee husks and corn cobs. They prepared the biosorbent modified CPE and performed square wave voltammetry (SWV) measurements for the detection of MB.

Florido et al. [26] performed the biosorption of Cu(II) ions using grape stalk wastes and analyzed the biosorption process by designing a flow injection system. They used flow-through tubular electrodes which were selective for Cu(II) ions and monitored the biosorption by potentiometry. They performed fixed-bed column experiments and experimental and predicted curves were obtained. The grape wastes were dried by applying 110 °C. Although the flow injection system allowed designing on-line measurement system, the preparation of the electrodes and implementation of the system required to use of extra chemical agents that increased the cost of the procedure and environmental burden.

To our present knowledge, there is no report in the literature for the application of disposable PGEs for monitoring of the biosorption process. This study aims (i) to perform PNL removal by using a biosorbent made by a factory waste and (ii) to determine PNL removal by a single-use voltammetric sensor. This is the first paper showing the application of a PGE-based voltammetric sensor to detect PNL removal by the biosorption process.

2 Material and Methods

2.1 Apparatus

IVIUM Compactstat.e with IVIUM Release 4.951 software package (The Netherlands) was used as the potentiostat to perform all electrochemical measurements. PGE was used as the working electrode in a three-electrode system (electrochemical cell). PGE was comprised of a graphite lead (Tombow, Japan) and a pencil (Rotring, Germany) holded a metallic wire. The graphite leads were obtained from local markets. 14mm of graphite lead was immersed into the solution for each electrochemical measurement. Other components of the electrochemical cell were a reference electrode (Ag/AgCl/3M KCl, BAS, Model RE-5B, W. Lafayette, USA) and a counter electrode as platinum wire.

2.2 Chemicals

PNL, 2,4-dichlorophenoxyacetic acid (2,4-D), and dimethyl sulfoxide (DMSO) were purchased from Sigma-Aldrich. Diclofenac sodium (DFC) and paracetamol (PRL) were purchased from the local drugstore. The stock solutions of PNL and 2,4-D were prepared as 1000 μg/mL in ultrapure water and in DMSO, respectively. The diluted solutions of PNL, 2,4-D, PRL, and DFC were prepared in ultrapure water (pH 1.00).

Other chemicals were obtained from Sigma-Aldrich and they were in analytical grade.

2.3 Preparation of the Biosorbent

The solid organic waste content used in the study consists of the pulp released after the lemon juice used during production in the factory is taken. This solid organic waste was used as a biosorbent in PNL removal experiments after drying. Solid organic waste from the Factory Production Facility (Figure S1a) was washed at least twice with pure water, dried at room temperature for 24 hours (Figure S1b), and then dried in an oven at 60 °C overnight (Figure S1c). After the room dried wastes are pulverized in mortar, they are stored in a refrigerator at +4 °C. During the biosorption experiments, the biosorbent obtained by drying from solid waste was passed through 150 μm porous sieves in order to use equal particle size [27].

2.4 Biosorption Studies

Various parameters for determining the optimal conditions for maximum PNL biosorption (pH (1.00–5.00); PNL concentration (5–100 μg/mL); temperature (5, 25 and 50 °C) and time (0–24 hours) effect experiments were examined with 1 g/L adsorbent dosage. Biosorption experiments were carried out in liquid environments containing a certain amount of PNL with a temperature and speed-controlled shaker stand. Then, samples of 10 milliliters were taken at specified time intervals and centri-

fuged at 10000 rpm for 5 minutes. The resulting supernatant was used for PNL determination. At each optimization step, the control experiments were done at the same experimental conditions for the biosorption of PNL but without adding PNL. The PNL control experiments were done at the same experimental conditions with the biosorption but without adding the biosorbent. The PNL biosorption rate (B%) was calculated from Equations (1) and (2);

$$\text{Biosorption rate } (B\%) = (C_o - C_f)/C_o \times 100 \quad (1)$$

$$q_m = C_o - C_f/X_m \quad (2)$$

q_m: the uptake of PNL by unit mass of biosorbent at any time (mg/g), C_o: initial PNL concentration (mg/L), C_f: final PNL concentration at any time (mg/L), X_m: the sorbent concentration (g/L).

For real sample analysis, pH values of drinking water and tap water samples were adjusted as pH = 1.00. Wastewater sample was obtained from the landfill leachate pool of a solid waste management facility in Çanakkale province (40°10′29″N 26°32′37″E) and 100 times diluted with the ultrapure water (pH 1.00).

2.5 Biosorption Isotherms and Kinetics

The common biosorption isotherm models such as Langmuir and Freundlich were examined in the current paper. The Equations of (3) and (4) were used for this reason.

$$\text{Langmuir Isotherm Equation : } C_e/q_e = (1/q_m)C_e + 1/K_L q_m \quad (3)$$

$$\text{Freundlich Isotherm Equation : } \ln(q_e) = \ln(K_F) + 1/n \ln(C_e) \quad (4)$$

q_m: the maximum capacity of adsorption (mg/g), K_L: Langmuir isotherm constant (L/mg), K_F: Freundlich isotherm constant (L/mg).

The most used kinetic models such as pseudo-first and second-order models were used to investigate the suitable kinetic model for biosorption studies. The equations of (5) and (6) were used.

$$\text{Pseudo-first-order kinetic model equation : } \log(q_e - q_t) = -k1/2.303\, t + \log q_e \quad (5)$$

$$\text{Pseudo-second-order kinetic model equation : } t/q_t = 1/k_2 q_e^2 + 1/q_e.t \quad (6)$$

q_e: The adsorption capacity (q_{ecal}: The theoretical adsorption capacity; q_{eexp}: The experimental adsorption capacity), k_1: rate constant of pseudo-first-order kinetic model, k_2: rate constant of pseudo-second-order kinetic model.

2.6 Electrochemical Measurements

Cyclic voltammetry (CV) measurements were performed during all studies. 1 mL of the sample obtained after the biosorption process was transferred into an electrochemical cell containing 1 mL 50 mM phosphate buffer solution (PBS; pH 7.40). The potential range was between +0.50 V to +1.20 V with the scan rate as 50 mV s^{-1} for all CV measurements. Before the biosorption process, the oxidation signal of PNL was measured at +1.020 V, +0.690 V, and +0.680 V at pH 1.00, 3.00, and 5.00, respectively. After the biosorption process, the oxidation signal of PNL was measured at +1.030 V, +0.800 V, and +0.800 V at pH = 1.00, 3.00, and 5.00, respectively.

2.7 FTIR and SEM Analyzes

In order to investigate the changes on the surface of biosorbent after PNL biosorption, Fourier Transform Infrared Spectroscopy (FTIR), Scanning Electron Microscope (SEM), and Energy-dispersive X-ray spectroscopy (EDX) analyzes were done with Agilent Technologies Cary 630 FTIR spectrophotometer and Leo 440 Computer Controlled Digital System, respectively. For all SEM and FTIR measurements, 1 g/L biosorbent and 15 µg/mL PNL were used. The biosorption process was done at pH 1.00 and 25 °C for 360 min. Then the samples were filtered, washed with distilled water, and allowed to dry overnight. The dried biosorbents (before and after biosorption) were powdered (blended with dry spectroscopic grade powders) and, then pressed into small disks for FTIR measurements. Samples were scanned at the scan range of 400–4000 cm^{-1}. SEM analyzes were performed at magnifications ranging from 500x to 5000x and the acceleration potential was 10 kV.

3 Results and Discussion

3.1 The Effect of pH and Shaking onto the Biosorption Process

The effects of pH and shaking were examined at pH 1.00, 3.00, and 5.00 in the presence of 50 µg/mL PNL for 24 hours (Figure 1 and Figure S2). The average PNL signals and the estimated B% values were given in Table S1. Maximum PNL removal could be obtained at pH 1.00 and shaking conditions (Figure 2A, a to b and Figure S2A, b to c) as 53.07 %. Further studies were performed at pH 1.00 and shaking conditions.

3.2 The Effect of PNL Concentration onto the Biosorption Process

The effect of PNL concentration upon the biosorption process was examined at the concentration level of PNL ranging from 5 to 100 µg/mL (Figure S3). Before the biosorption process, the average PNL oxidation signal was measured as 1.26 (Figure S3A, a) and 3.16 µA (Fig-

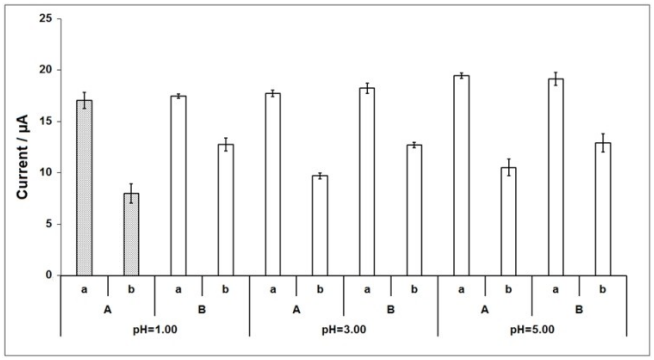

Fig. 1. Histograms representing the average PNL signals (n = 3) obtained before **(a)** and after **(b)** the biosorption process performed at shaking **(A)** or static **(B)** conditions and different pH values ranging from 1.00 to 5.00. (Initial PNL concentration: 50 µg/mL; T: 25 °C, Contact time: 24 h).

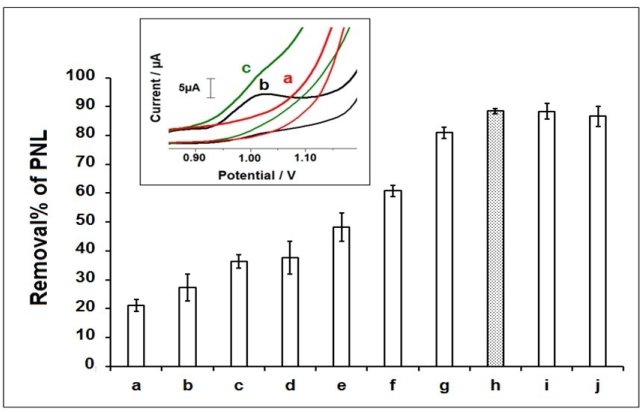

Fig. 2. Histograms representing the average removal% values of PNL obtained after 15 **(a)**, 30 **(b)**, 45 **(c)**, 60 **(d)**, 90 **(e)**, 120 **(f)**, 240 **(g)**, 360 **(h)**, 480 **(i)** min and 24 h **(j)** biosorption. Inset is the voltammograms representing biosorbent control **(a)**, PNL oxidation signal before **(b)** and after **(c)** 360 min biosorption. (Initial PNL concentration: 15 µg/mL; pH = 1.00, T: 25 °C).

ure S3A, b) with the relative standard deviation values % (RSD%) as 13.70 % and 7.00 % at 5 and 10 µg/mL concentration level of PNL, respectively. No PNL signal was observed after the biosorption of 5 and 10 µg/mL PNL which meant that the removal of PNL was successfully achieved at the low concentration level of PNL. B% values were calculated as 88.77 %, 64.68 %, 66.94 %, 50.70 %, 51.28 % and 47.94 % at 15, 20, 25, 50, 75 and 100 µg/mL concentration level of PNL, respectively. As it can be seen, the PNL oxidation signal increased during the concentration of PNL increased and no saturation could be observed at the PNL signal. Therefore, the lowest concentration level of PNL allowed the monitoring of the PNL signal after the biosorption process was chosen and 15 µg/mL PNL was used for further studies.

3.3 The Effect of Temperature onto the Biosorption Process

To examine the effect of temperature on PNL removal by waste biosorbent, the experiments were performed at 5, 25, and 50 °C (Figure S4). Before the biosorption at 5, 25, and 50 °C (Figure S4A, a to c), the average PNL signals were found to be 7.27, 5.22, and 6.98 µA with the RSD% values as 3.06 %, 13.57 %, and 10.81 %, respectively (n = 3). After the biosorption at 5, 25, and 50 °C (Figure S4B a' to c'), B% values were estimated as 56.39 %, 88.77 %, and 75.28 %, respectively. 25 °C was chosen as optimum for the biosorption due to the highest removal of PNL could be observed at this temperature level.

3.4 The Effect of Contact Time onto the Biosorption Process

The biosorption process was performed during different contact times from 15 min to 24 h in order to investigate the effect of contact time upon the sensor response. Figure 2 represents the average B% values obtained using different contact times. The average B% value increased till 360 min contact time (Figure 2h) and almost no change at the average B% value was observed at higher contact time. The average PNL signals were measured as 4.53 and 0.52 µA (RSD% values as 6.90 % and 8.10 %, n = 3) before and after 360 min biosorption, respectively. PNL removal was calculated as 88.42 % (Figure 2, inset, b to c) after 360 min biosorption, and next studies were done during this contact time.

Sihem et al. [28] reported that the adsorbent obtained from the local cereal by-products removed 70 % of PNL by 2 hours maximally. Before investigating the PNL removal performance of the waste solid material they applied a pretreatment process for preparing adsorbent (calcined at 600 °C), which was both energy and time consuming, and reached 70 % PNL removal performance. In the current study, the bio-based solid waste was used directly (without any pre-treatment process) and achieved 82.42 % PNL removal rate.

3.5 Electrochemical Investigation of the Biosorption in Real Samples

In order to show the applicability of the sensor system into real sample analysis, the biosorption process was performed into tap water, drinking water, and wastewater samples under optimum conditions, then the biosorption process was monitored by the voltammetric sensor system (Figures 3, S5). The average PNL signals and the B% values were calculated as 74.46 %, 73.58 %, and 72.06 % in drinking water, tap water, and wastewater samples. Although a small decrease at the B% value was observed in the real samples, these results showed that the biosorption process of PNL could be successfully monitored by using the voltammetric sensor.

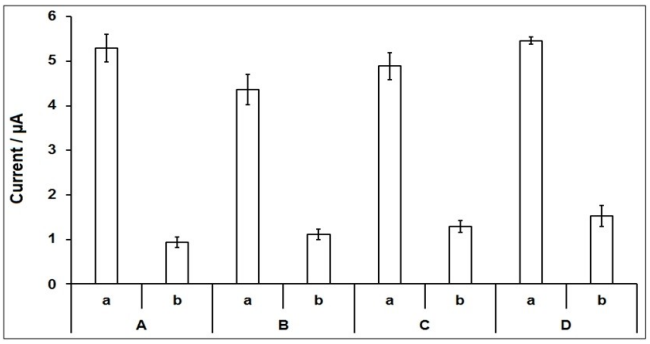

Fig. 3. The average PNL signals obtained before **(a)** and after **(b)** the biosorption in the presence of ultrapure water **(A)**, drinking water **(B)**, tap water **(C)** and wastewater **(D)** (n = 3).

The effect of the presence of other phenolic compounds on the biosorption process was tested by using the developed voltammetric sensor system (Figure 4). For this purpose, the biosorption of PNL was performed in the presence of the mixture of 15 µg/mL: 15 µg/mL PNL:PRL, PNL:2,4-D, and PNL:DFC. There were oxidation signals coming from 15 µg/mL PRL and 15 µg/mL DFC measured at +0.66 V (Figure S6–a) and +0.83 V (Figure S6–c), respectively and 2,4-D did not give any oxidation signal (Figure S6-b). The oxidation signals of PRL and DFC did not overlap with the PNL signal (Figure S7). Therefore, decreases at the PNL signal obtained before/after the biosorption process were evaluated in the presence of the interference factors. The B% values were calculated as 82.27 %, 82.01 %, 80.28 % and 87.12 % in the presence of 15 µg/mL PNL or 15 µg/mL:15 µg/mL PNL:PRL, PNL:2,4-D, and PNL:DFC, respectively (Table S3). It could be concluded that the presence of the interference factors did not affect the biosorption process and the electrochemical monitoring of the PNL biosorption by using disposable PGEs.

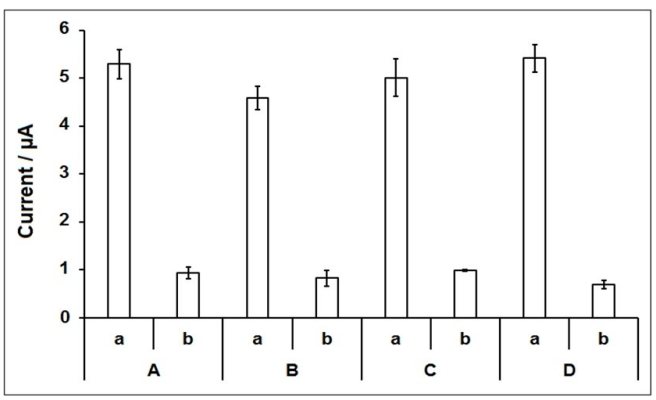

Fig. 4. The average PNL signals obtained before **(a)** and after **(b)** the biosorption process occurred in the presence of 15 µg/mL PNL **(A)** or 15 µg/mL:15 µg/mL PNL:PRL **(B)**, PNL:2,4-D **(C)** and PNL:DFC **(D)** (n = 3).

Within the scope of the present manuscript, an innovative electrochemical approach was introduced into the biosorption area for the first time. This electrochemical system has crucial properties such as being an eco-friendly, time-saver, practical, and having the on-line measurement capability that makes it preferable to the other analytical tools. The usage of factory waste for the biosorption process allowed to design of sustainable and recyclable monitoring systems. The PNL removal was achieved at room temperature without any chemical treatment that required minimum investment cost for future scale-up studies. The use of PGE for the monitoring of the PNL removal provided to fabricate a practical, cheap, and accessible detection platform. It should be emphasized that the use of PGE did not require any electrochemical or chemical pretreatment or activation step, it was bought from the local market and used for electrochemical measurements by just dipping the measurement solution. Moreover, each electrochemical measurement was completed in just 40 s by using the CV technique. All experiments were performed at 15 µg/mL concentration level of PNL which was quite higher than the one reported by the European Union as acceptable PNL concentration level in drinking water [29]. In addition to all advantages said above, reproducible sensor response was obtained by using single-use PGE-based electrochemical sensor system which is the another crucial property for the development of a (bio)sensor system.

Although there have been numerous reports in the state-of-art about PNL removal by the biosorption process [30–34], there is no report in the literature about the integration of disposable electrochemical sensor systems into the biosorption area. It is expected that this study will lead to the design of novel detection routes for PNL biomonitoring into contaminated water samples. Since environmental pollution has been increasing day-by-day and phenolic compounds have been a big part of the pollutants, there are a tremendous number of reports for electrochemical detection of PNL and phenolic compounds [35–41]. This study will bring a new perspective into the electrochemical biomonitoring area whose applications are focused on the recognition of PNL or phenolic compounds.

3.6 Biosorption Isotherms

Biosorption isotherms were calculated with a biosorbent which was the most efficient biosorbent and given in Table 1. The correlation values of Langmuir and Freundlich isotherms were calculated as 0.975 and 0.977 for the biosorption of PNL on waste biosorbent, respectively. Similarly the PNL removal efficiencies of wastes-Rice mill residue (RM), Wheat mill reside (WM), Dall mill residue (DM), and the Banana peels (BM) were investigated and the PNL biosorption was suitable with the Freundlich isotherm model for all solid wastes and the maximum PNL removal capacity was found to be 6.189 mg/g [42]. Due to the highest correlation value, the Freundlich

Table 1. Langmuir and Freundlich constants for PNL biosorption by waste biosorbent (q_m: the maximum capacity of adsorption; K_L: Langmuir isotherm constant; K_F: Freundlich isotherm constant).

	Langmuir			Freundlich		
	q_{max} mg/g)	K_L (L/mg)	R^2	K_F (L/mg)	1/n	R^2
Waste biosorbent	9.52	1.06	0.975	36.198	0.964	0.977

isotherm model is suited with the biosorption of PNL on the biosorbent (Table 1). This result showed that the PNL biosorption onto waste biosorbent was a heterogeneous process [43].

3.7 Biosorption Kinetics

The correlation of the pseudo-first-order model was 0.962 and the experimental $q_{e\ exp}$ (33.70 mg/g) value was not near the calculated q_{ecal} (13.97 mg/g). For the pseudo-second-order model, the correlation was higher than the correlation for the pseudo-first-order 0.977 and the experimental q_e (33.70 mg/g) and calculated q_e (33.33 mg/g) values were very close, so the PNL biosorption on the waste biosorbent was suitable with the pseudo-second-order kinetic model (Table 2). Recently, Kumar et al. [44] showed that the adsorption of PNL compounds by waste fruit shell originated adsorbent was compatible with the pseudo-second-order kinetic model. The results of the kinetic model calculations of the current paper were fitted with the recent literature results.

3.8 FTIR Analysis

In order to have more information about the PNL biosorption properties of waste biosorbent, the PNL treated and untreated biosorbent samples were analyzed with FTIR and the FTIR spectra of waste biosorbent before and after biosorption were given in Figure S8-a and b, respectively. When the FTIR spectra of biosorbent before (Figure S8a) and after (Figure S8b) biosorption of PNL were examined, after PNL treatment the new peak at 889.89 cm^{-1} appeared. Khaskheli et al. [45] stated that the new peak formation at FTIR spectra of lemon peel after metal adsorption is revealed to oxygen metal bond. Also recently, Zhuang et al. [46] the band observed at 896 cm^{-1} in the spectrum of biomass indicated the C–O–C stretching due to the cellulose. The major differentiation of FTIR spectra of PNL unloaded (Figure S8a) and loaded (Figure S8b) biosorbent occurred between 1000 and 1200 cm^{-1} regions. The peak at 1012.51 cm^{-1} shifted to 1016.16 cm^{-1} and the new peak formations were observed at 1101.34 and 1147.97 cm^{-1}. In general, the characteristic peaks of phenols appeared at the region between 1000 and 1200 cm^{-1} in FTIR analysis [47]. The significant and major shifts were assumed as indicative of the interaction between PNL and the functional groups of the biosorbent surface. Previously, Arslanoglu et al. [48] reported that the peaks at 1000–1200 cm^{-1} region related to the characteristic cellulose peaks in the FTIR spectra of lemon peel. According to this information, the shift of the peak at 1012.5 to 1016.16 observed in the FTIR spectrum of the biosorbent after PNL treatment indicates that some groups in the cellulose interact with PNL. Khaskheli et al. [45] used orange peel (structurally similar to lemon peel) as a biosorbent, stated that the peak shifting from 1011.21 cm^{-1} to 1016 cm^{-1} in the FTIR spectrum after biosorption indicates C–O bonding. Recently, Zhuang et al. [46] reported that the FTIR band at 1160 cm^{-1} represents the C–O-C stretching of cellulose found on the surface of biomass. The peak observed at 1437.29 shifted to 1441.74 cm-1 after PNL biosorption. The peak at 1440 assigned (C–C) aromatic (conjugated with C=C) related with phenolic compounds [49]. Berezin et al. [50] reported that the FTIR band at 1630 cm^{-1} related to the vibrations of C=C bonds of the conjugated carbon rings. In addition to this, the peak at 1650 cm^{-1} observed in the FTIR spectrum of lemon peel indicates the C–O stretching vibration of carboxylic acids related to the carboxyl groups of cellulose [50]. In the FTIR results of this study, the peak at 1611.03 cm^{-1} of PNL unloaded biosorbent shifted to 1628.23 cm^{-1} of PNL loaded biosorbent (Figure S8). The change at FTIR bands may cause by the interactions between PNL and the functional groups at the surface of the biosorbent due to the present carbon rings on the surface. The peak appeared at 1611.03 cm^{-1} shifted to 1628.23 cm^{-1} after PNL sorption, indicated the involvement of ν (C=C) Phenolic acid formation in the biosorption process [49]. The bands at the 2800–3000 cm^{-1} region indicated the stretching of C–H bonds in the saturated carbon rings of polysaccharides [50]. According to the results of FTIR analysis, the

Table 2. Kinetic parameters for the biosorption of PNL onto waste biosorbent (q_{ecal}: The theoretical adsorption capacity; q_{eexp}: The experimental adsorption capacity; k_1: rate constant of the pseudo-first-order kinetic model, k_2: rate constant of the pseudo-second-order kinetic model).

	Pseudo-first-order model				Pseudo-second-order model			
	qe_{cal}	qe_{exp}	k_1	R^2	qe_{cal}	qe_{exp}	k_2	R^2
Waste biosorbent	13.97	33.70	0.6909×10^{-3}	0.962	33.33	33.70	1424.44	0.976

major difference at FTIR peaks was observed at 2800–3000 cm^{-1} region (Figure S8). When all the previously mentioned literature information and the FTIR results obtained from this study are examined; During biosorption, the phenomenon that PNL interacts with the C–O–C functional groups in the cellulose part of the lemon peel forming the biosorbent has been confirmed.

3.9 SEM and EDX Analyzes

Before and after PNL biosorption analyzes, biosorbent characterization was performed by SEM technique (Figure 5) [51–54]. In Figure 5-A, the porous structure of the biosorbent was seen in the images obtained from all magnifications. This porous structure may be attributed to the organic structure of the biosorbent [55]. After PNL biosorption (Figure 5-B), the angular and recessed-protruding structure of the biosorbent turned into more fibrous and soft lines. The elemental concentrations of oxygen and carbon atoms obtained by EDX analysis were represented in Table 3. Weight% of carbon atom decreased after PNL adsorption while weight % of oxygen atom increased after PNL adsorption. SEM and EDX results confirmed the FTIR results and showed carbon and oxygen atoms had a role in the biosorption process. All results showed that PNL removal can be successfully performed by using the waste biosorbent.

4 Conclusion

Herein, an electrochemical sensor system for monitoring the PNL removal was reported for the first time in the literature. First, the PNL removal was done by using a factory waste biosorbent, then the electrochemical detection of the PNL from the samples obtained before/after the biosorption process was performed. The changes at the oxidation signal of PNL were evaluated for the evaluation of the biosorption. Effective binding of the PNL molecules on the biosorbent was monitored using SEM and FTIR techniques. PGE based design of the voltammetric sensor system provided to fabricate a low cost, practical, time saver, and eco-friendly analytical tool,

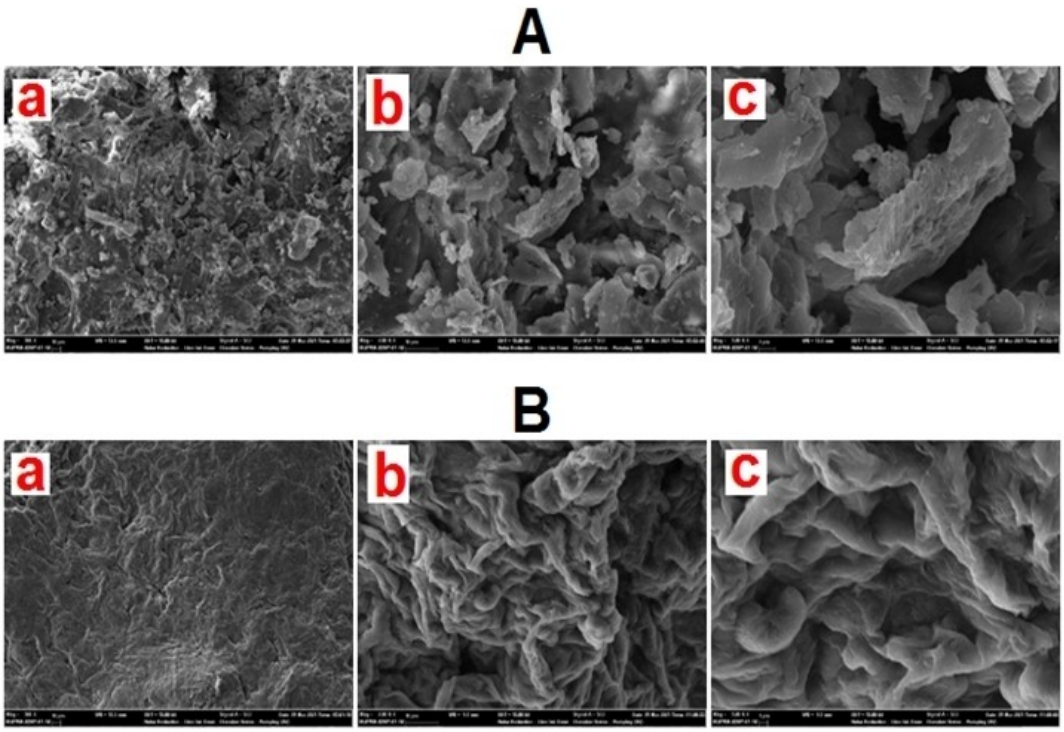

Fig. 5. SEM images of the biosorbent before (A) and after (B) biosorption performed in the presence of 15 µg/mL PNL during 360 min at pH = 1.00 and 25 °C. Magnifications of SEM analyzes are 500x (a), 2000x (b) and 5000x (c). The acceleration potential is 10 kV.

Table 3. The elemental composition (%) of carbon and oxygen atoms of the biosorbent obtained before and after the biosorption process at optimal conditions (PNL Concentration: 15 µg/mL; contact time: 360 min.; pH: 1.00 and temperature: 25 °C).

Biosorbent	Carbon (wt.%)	(at.%)	Oxygen (wt.%)	(at.%)	Total (wt.%)	(at.%)
Before biosorption	53.22	60.25	46.78	39.75	100	100
After biosorption	47.38	54.53	52.62	45.47	100	100

and the PNL removal was performed with a minimum environmental burden as well as the development of the monitoring system. This study will lead to fabricate new miniaturized detection platforms that have a great capacity for online measurements without the necessity of the application of complex experimental procedures. Also, this study has a big potential for being an origin for the development of novel electrochemical (bio)sensor platforms that will aim to monitor different types of environmental pollutants.

Acknowledgements

This study was supported by Bilecik Seyh Edebali University Scientific Research Project Coordination (Project number: 2020-01.BŞEÜ.12-02).

Data Availability Statement

Author elects to not share data- Research data are not shared.

References

[1] S. Noh, H. Yang, *Electroanalysis* **2014**, *26*, 2727–2731.
[2] A Rana, A. N. Kawde, *Electroanalysis* **2016**, *28*, 898–902.
[3] Q. Xie, J. Cao, D. Sun, H. Lu, M. Xia, B. Hou, D. Li, L. Jia, *J. Mol. Liq.* **2020**, *303*, 112501.
[4] Y. Ma, N. Gao, W. Chu, C. Li, *Front. Environ. Sci. Eng.* **2013**, *7*, 158–165.
[5] N. Singh, C. Balomajumder, *Water Conservation Sci. Eng.* **2017**, *2*, 1–14.
[6] I. Senturk, H. Buyukgungor, *Ekoloji* **2013**, *22*, 1–12.
[7] I. Senturk, H. Buyukgungor, F. Geyikci, *Desalin. Water Treat.* **2015**, *57*, 19529–19539.
[8] L. G. C. Villegas, N. Mashadi, M. Chen, D. Mukherjee, K. E. Taylor, N. Biswas, *Curr. Pollution Rep.* **2016**, *2* 157–167.
[9] S. Ertugrul Karatay, Ü. D. Gül, G. Dönmez, *J. Surfactants Deterg.* **2014**, *17*, 1223–1228.
[10] F. Piroozmand, F. Mohammadipanah, F. Faridbod, *Synth. Syst. Biotechnol.* **2020**, *5*, 293–303.
[11] A. M. Stortini, M. A. G. Baldo, F. Moro, L. Polo, L. M. Moretto, *Sensors* **2020**, *20*, 6800.
[12] L. Fang, X. Liao, B. Jia, L. Shi, L. Kang, L. Zhou, W. Kong, *Biosens. Bioelectron.* **2020**, *164*, 112255.
[13] P. S. Sfragano, S. Laschi, I. Palchetti, *Front. Chem.* **2020**, *8*, 644.
[14] S. Tajik, H. Beitollahi, F. G. Nejad, Z. Dourandish, M. A. Khalilzadeh, H. W. Jang, R. A. Venditti, R. S. Varma, M. Shokouhimehr, *Ind. Eng. Chem. Res.* **2021**, *60*, 3, 1112.
[15] S. Tajik, Y. Orooji, F. Karimi, Z. Ghazanfari, H. Beitollahi, M. Shokouhimehr, R. S. Varma, H. W. Jang, *J. Food Meas. Charact.* **2021**, *15*, 4617.
[16] Y. Orooji, P. N. Asrami, H. Beitollahi, S. Tajik, M. Alizadeh, S. Salmanpour, M. Baghayeri, J. Rouhi, A. L. Sanati, F. Karimi, *J. Food Meas. Charact.* **2021**, *15*, 4098.
[17] B. Pérez-Fernández, A. Costa-García, A. Escosura-Muñiz, *Biosensors* **2020**, *10*, 32.
[18] Annu, S. Sharma, R. Jain, A. N. Raja, *J. Electrochem. Soc.* **2019**, *167*, 037501.
[19] G. Congur, Ü. D. Gül, *J. Environ. Chem. Eng.* **2021**, *9*, 105804.
[20] A. Rana, N. Baig, T. A. Saleh, *J. Electroanal. Chem.* **2019**, *833*, 313–332.
[21] I. G. David, D. E. Popa, M. Buleandra, *J. Anal. Method. Chem.* **2017**, 1905968.
[22] I. G. David, I. A. Badea, G. L. Radu, *Turk. J. Chem.* **2013**, *37*, 91.
[23] L. Cao, Z. W. Kang, Q. Ding, X. Zhang, H. Lin, M. Lin, D. P. Yang, *Sci. Total Environ.* **2020**, *723*, 138008.
[24] J. Estrada-Aldrete, J. M. Hernández-López, A. M. García-León, J. M. Peralta-Hernández, F. J. Cerino-Córdova, *J. Electroanal. Chem.* **2020**, *857*, 113663.
[25] E. Njanja, S. F. Mbokou, M. Pontie, M. Nacef, I. K. Tonle, *SN App. Sci.* **2019**, *1*, 513.
[26] A. Florido, C. Valderram, S. Nualart, L. Velazco-Molin, O. Arias de Fuentes, M. del Valle, *Anal. Chim. Acta* **2010**, *668*, 26–34.
[27] Ü. D. Gül, S. İlhan, C. Filik İşçen, *J. Surfactants Deterg.* **2019**, *56*, 188–196.
[28] A. Sihem, M. Bencheikh Lehocine, H. A. Miniai, *Energy Procedia* **2012**, *18*, 1135–1144.
[29] P. Önnerfjord, J. Emneus, G. Marko-Varga, L. Gorton, F. Ortega, E. Dominguez, *Biosens. Bioelectron.* **1995**, *10*, 607–619.
[30] N. Singh, A. Kumari, C. Balomajumder, *Saudi J. Biol. Sci.* **2018**, *25*, 1454–1467.
[31] G. L. Dotto, J. A. V. Costa, L. A. A. Pinto, *J. Environ. Chem. Eng.* **2013**, *1*, 1137–1143.
[32] G. L. Dotto, J. O. Gonçalves, T. R. S. Cadaval, L. A. A. Jr. Pinto, *J. Colloid Interface Sci.* **2013**, *407*, 450–456.
[33] N. Singh, C. Balomajumder, *J. Environ. Chem. Eng.* **2016**, *4*, 1604–1614.
[34] V. Farkas, A. Felinger, A. Hegedűsov, I. Dékány, T. Pernyeszi, *Colloids Surf. B* **2013**, *103*, 381–390.
[35] M. Nurdin, L. Agusu, A. A. M. Putra, M. Maulidiyah, Z. Arham, D. Wibowo, M. Z. Muzakkar, A. A. Umar, *J. Phys. Chem. Solids* **2019**, *131*, 104–110.
[36] M. H. Aliabadi, N. Esmaeili, H. S. Jahromi, *App. Nanosci.* **2020**, *10*, 597–609.
[37] W. Qin, X. Liu, H. Chen, J. Yang, *Anal. Methods* **2014**, *6*, 5734.
[38] S. Sakthinathan, S. Palanisamy, S. M. Chen, P. S. Wu, L. Yao, B. S. Lou, *Int. J. Electrochem. Sci.* **2015**, *10*, 3319–3328.
[39] G. Pan, G. Zhao, M. Wei, Y. Wang, B. Zhao, *Chem. Phys. Lett.* **2019**, *732*, 136657.
[40] Y. Yan, X. Bo, L. Guo, *Talanta* **2020**, *218*, 121123.
[41] T. S. Cheng, M. Z. Mohamad, N. A. Ambrosi, M. Pumera, *App. Mater. Today* **2017**, *9*, 212–219.
[42] C. R. Girish, V. Ramachandramurty, *J. Environ. Sci. Eng.* **2013**, *55*, 275–282.
[43] L. Tabana, S. Tichapondwa, F. Labuschagne, E. Chirwa, *Sustainability* **2020**, *12*, 4273.
[44] N. S. Kumar, H. M. Shaikh, M. Asifl, E. H. Al-Ghurabi, *Sci. Rep.* **2021**, *11*, 2586.
[45] M. I. Khaskheli, S. Q. Memon, A. N. Siyal, M. Y. Khuhawar, *Waste Biomass Valorization* **2011**, *2*, 423–433.
[46] J. Zhuang, M. Li, Y. Pu, A. J. Ragauskas, C. G. Yoo, *Appl. Sci.* **2020**, *10*, 4345.
[47] P. Larkin, Infrared and raman spectroscopy principles and spectral interpretation. 2011, Elsevier, Amsterdam, The Netherlands.
[48] H. Arslanoglu, H. S. Altundogan, F. Tumen, *Bioresour. Technol.* **2008**, 99, 2699.

[49] J. A. Heredia-Guerrero, J. J. Benítez, E. Domínguez, I. S. Bayer, R. Cingolani, A. Athanassiou, A. Heredia, *Front. Plant Sci.* **2014**, *5*, 305.
[50] K. V. Berezin, I. T. Shagautdinova, M. L. Chernavina, A. V. Novoselova, K. N. Dvoretskii, A. M. Likhter, *Opt. Spectrosc.* **2017**, *123*, 495.
[51] Z. M. Şenol, Ü. D. Gül, R. Gürkan *J. Env. Health Sci. Eng.* **2020**, *29*, 853.
[52] Ü. D. Gül, E. İrdem, Ş. A. Yavuz, S. İlhan, *J. Text. Inst.* **2021**. *112*, 1014.
[53] K. Jeddou, F. Bouaziz, F. B. Taheur, O. Nouri-Ellouz, R. Ellouz-Ghorbel, S. Ellouz-Chaabouni, *Water Sci. Technol.* **2021**, *83*, 1384.
[54] L. B. L. Lima, N. Priyantha, Y.-C. Lu, N. A. H. M. Zaidia, *Desalin. Water Treat.* **2019**, *166*, 44.
[55] J. O. Ighalo, A. G. Adeniyi, *SN App. Sci.* **2020**, 2, 509.

Received: September 30, 2021
Accepted: October 21, 2021
Published online on November 19, 2021

